Fachtagung "Lasermethoden in der Strömungsmesstechnik"
9. – 11. September 2014, Karlsruhe

Mehrskalen Untersuchung turbulenter Parameter in einer Blasensäule mithilfe optischer Separation mehrerer Laserschnitte.

Multiscale investigations of turbulent parameters in a big scale bubble column using optical discrimination of multiple laser planes.

B. König, S. Puttinger, S. Pirker
Christian Doppler Laboratory on Particulate Flow Modelling, Johannes Kepler Universität Linz, Altenbergerstrasse 69, 4040-Linz, Austria. bernhard.koenig@jku.at

Optische Trennung, Blasensäule, Mehrskalen Turbulenz, alternierende Spülung, Konverter
laser separation, converter, alternating aeration, rinsing of liquid metal,

Abstract
A multiscale experimental procedure is introduced permitting the investigation of a special area of interest simultaneously to the global view of a 0.91x1x0.5m bubble column. The area of interest is acquired at a higher time and spatial resolution to achieve more accurate measures of the turbulent parameters. Discrimination of the global view and the magnification area is realised by the use of two lasers, emitting different wavelengths, and corresponding optical filters in front of the dedicated cameras. Since the two phase flow would introduce problematic conditions for the PIV algorithms a masking scheme for separating both phases is illustrated.

Introduction
Bubble stirred flows or bubbling beds are commonly known for several industrial processes in multiple fields and purposes like for example mixing and homogenisation. Within steel production bubble columns are used for desulphurisation by rinsing the liquid metal with nitrogen where the triggered convective flow and turbulences therein contribute directly to the effectiveness of the process. Usually the industrial columns are equipped with one or several porous plugs located near the bottom centre and operated simultaneously. To increase the mixing behaviour recent developments investigate multiple porous plugs which are alternately activated. Hence, the understanding of the turbulent structures formed within the column and the influencing parameters are essential to increase the efficiency even further.

The measurement and proper analysis of turbulent quantities within their full spectrum is related to a high temporal and spatial resolution. In recent years several methods have received significant attention and are developed to high levels. Two-phase flows, and especially air-water flows, are the system of interest herein and only methods applicable in this dedicated field are introduced. An overall review of measurement techniques within gas-liquid and gas-liquid-solid reactors can be found in Boyer et al. 2002. In such systems the acquisition is aggravated due to strong discontinuities in the physical variables used to sense the flow. For instance optical methods like Particle Image Velocimetry (PIV), Laser Doppler Anemometry (LDA), and Phase Doppler Anemometry (PDA) are hampered by the optical diffraction and refraction of the dispersed bubbles and are therefore limited to relative small gas hold ups.
Techniques which are insensible to these limitations are for example the computer-automated-radioactive-particle-tracking (CARPT) or computer tomography (CT) systems. The CARPT technique, originally developed by Lin et al. 1985 for solids motion in fluidised

beds, introduced to liquid motion in Devanathan et al. 1990 and further investigated in the Ph.D. thesis of Devanathan 1991. Utilizing a radioactive material encapsulated within a synthetic housing which is tracked by several γ radiation sensors over a long period of time (~20h). A problem with CARPT is the lack to measure velocities at two separated positions synchronously[1] since it represents a Lagrangian technique with only one tracer.

Tomographic techniques often use medical equipment and are based on X-rays (Seeger et al. 2001), γ -rays (Kumar et al. 1996), magnetic resonance (Elkins et al. 2007) or electrical capacitance (Huang et al. 1988 and 1989). Usually these systems contain a source (fan beam source for X- and γ - ray or RF pulse coil for magnetic resonance) located at the opposite side (or several electrodes as transmitter and receiver) of a sensor array acquiring a slice of the test section. These configurations can be rotated around the axis, enabling different viewing angles, and transversed axially to yield 3d data. Those procedures are not hindered by high gas holdups nor by opaque liquid conditions, but beyond the enormous costs and complexity of such systems the rather weak time and/or spatial resolution for the targeted bubble column size remains.

Point measurement techniques like LDA (Becker et al. 1999, Kulkarni et al. 2007, Mudde et al. 1998 and 2001) and PDA (Lain et al. 1990 or Brenn et al. 2002) are often mentioned in former but also recent researches. The great temporal resolution enables them to serve as a reference for other methods like PIV (see e.g. Deen et al. 2000) but as it is a single point measurement the desired spatial resolution is not achieved without inadequate effort. The same argument holds for hot wire probes or hot film anemometry applied for example by Chen et al. 2001 or Garnier et al. 2002.

In order to acquire a solid base for the statistical analysis both phases should be captured over the whole domain while maintaining adequate resolution in time and space. PIV as standalone but also in combination with shadowgraphy is able to fulfil these criteria and is in contrast to tomographic techniques rather inexpensive and easy to handle. The main limitation is its restriction to low gas hold ups typically around 10%, but also hold ups of 19% are reported in literature for instance by Bröder and Sommerfeld 2002 utilising a physical effect of different scattering modes to discriminate both phases. By using an additional optical filter and fluorescent seeding (light induced fluorescence, LIF) they were able to improve the results even further. As this representative example indicates, PIV is able to capture both phases simultaneously which is rarely possible with other techniques.
The main difference in most of the literature concerning PIV is the type of separation procedure used to discriminate the phases. Several methods are reviewed in the paper of Sathe 2010 and the basic principles shall also be mentioned here.

Single camera systems:
Most of these systems are based on image processing algorithms and separate the phases by either:

- size (Tracer particles are very small compared to bubbles) or
- slip velocity (Bubbles rise faster than fluid which can be detected by second correlation peaks (see Delnoij 2000)) or
- colour/grey gradient differences when using simultaneous shadowgraphy (see for example Lindken 2002 and Bröder and Sommerfeld 2007)

To separate out of focus bubbles acquired from the shadowgraphy a narrow depth of focus lens is deployed. Bubbles out of focus then appear with blurred edges and therefore can be detected by the algorithm.

[1] This would be interesting for calculating turbulent length and time scales for example.

Multi camera systems:

These designs frequently use optical separation like fluorescent tracer particles (LIF) and optical filters[2]. Several principles of multi-camera systems are reported in the Literature and recent developments point in the direction of resolving bubble trajectories and/or fluid movement three dimensionally (as a representative Brücker 1999 and Belden 2012 should be mentioned). As most of these principles are enhancements of 2d techniques the prevalent reported setups are illustrated in Fig. 1. The setup depicted in Fig. 1 (a) represents an usual PIV/LIF arrangement with optical separation by means of corresponding filters in front of the cameras. The main drawback of this setup is that even if the high intense reflections of the bubbles are mostly damped, they are still clearly visible on the captured image of the fluid flow camera due to reflections of the frequency shifted light emitted by the tracer particles and their accumulation at the bubble surface. As mentioned before by a smart choice of the observation angle Bröder and Sommerfeld 2002 reduced this effect. Arrangements like illustrated in Fig. 1 (b) and (c) are also realized without shadowgraphy as can be found in Kück et al. 2009 or Deen et al. 2000 respectively. The benefit of applying shadowgraphy is that bubble circumferences within the focus area are mapped sharply. Using merely LIF separation may lead to images of bubbles which are not closed (u-shaped) as a result of reflection and refraction effects within the bubble or shadowing of the lightsheet. This represents a local lack of information and needs to be considered by the post processing algorithm. Shadowgraphy eliminates this effect but runs into problems at dense bubble fractions since a shadow is generated for every bubble over the whole depth of the column and not only within an illuminated light sheet[3]. This yields a lot of virtually 'agglomerated' bubbles which cannot be separated easily applying the gradient of grey values. As the herein used physical depth of the experimental facility is large (between 0.5-1m) and the depth-of-focus of the available optics is unfeasible, the shadowgraphy procedure runs into problems and is therefore not used.

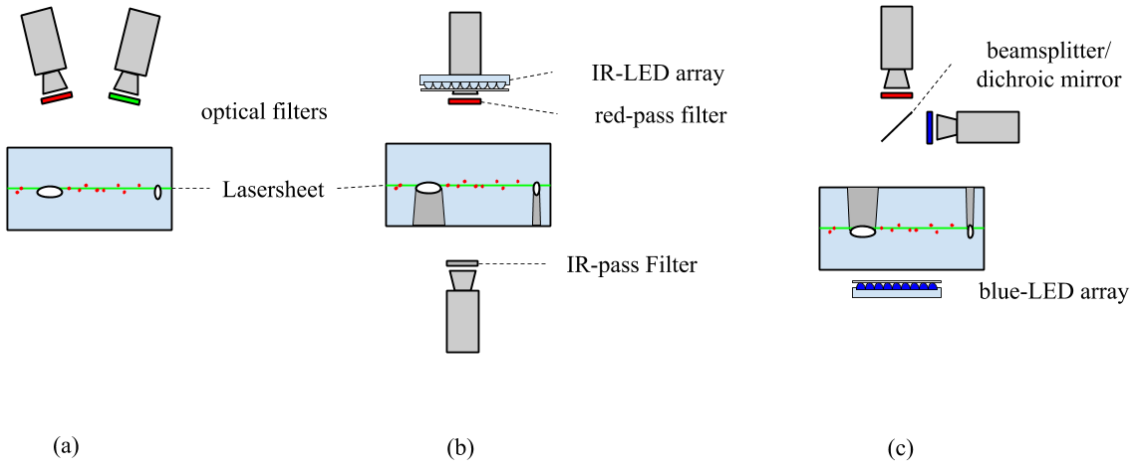

Fig. 1: Multi camera setups used to discriminate liquid and gas phase. (a) Setup used by Bröder and Sommerfeld 2002**,** (b) used an infrared shadowgraphy and LIF by Tokuhiro et al. 1998, (c) Sathe et al. 2010 used a blue LED array to enhance the background (like mentioned in Lindken 2002) and a dichroic mirror with adjacent filters for separation.

[2] Which are also usually used in single camera systems to block, or at least damp, the high intensity reflections of the bubbles.

[3] Certainly the narrow depth of focus lens will blur out of focus bubbles rapidly with increasing distance to the focal plane but nevertheless a considerable region remains.

Methods

Experimental apparatus:

The measurement setup was chosen according to the considerations of the previous section and is illustrated in Fig. 3. As the measurement and proper analysis of the detailed turbulent quantities is related to a high temporal and spatial resolution, PIV techniques are well suited for measurements. The industrial system of nitrogen and liquid-metal is commonly substituted by an air-water lab-scale experiment. The experimental column dimensions are 1m wide, 0.83m high and 0.5m in depth. The two porous plugs are located at x=250 and 750mm, centred in depth at z=-250mm with the coordinate systems origin at the left bottom (see Fig. 3). The aeration area of each plug is 40x40mm and is activated alternately for 78 seconds with a volume flow rate of 16 standard litres per minute. The porous media introduces heterogeneous bubble diameters[4] between 3mm and 12mm with its size distribution maximum at around 5mm. Note that this is just a rough estimation due to evaluation only within a 2d slice of few images and is mentioned solely for getting a better overview of the input parameters.

To achieve a reasonable spatial resolution of the global flow field the illuminated x-y plane (at z=-200mm depth) needs to be monitored by two cameras (Cam1 and Cam2 in Fig. 3). To reduce the data-loss caused by the dense bubble swarm the recording plane was set 50mm in front of the aeration plugs. This was thought as an acceptable trade-off between data-loss and mid-plane observation. These two cameras (LaVision Imager Intense) are double-frame cameras synchronized with a frequency doubled Nd:YAG laser, emitting two green light (532nm) pulses separated with a dedicated dt=30ms at a maximal repetition rate of 4Hz. Both cameras have a scaling ratio of 1.35 px/mm. To permit the observation of smaller turbulent time- and length-scales in a special area of interest a third high resolution camera (Point-Grey Grasshopper 3) and a blue (445nm) continuous wave laser are added. The blue laser is adjusted to illuminate the same plane as the Nd:YAG laser pulses and is recorded by Cam3 in Fig. 3 at a frame rate of 12fps. An optical blue pass filter is attached to this camera to achieve a constant illumination over all frames[5] while Cam1 and Cam2 are equipped with a green pass filter.

Since turbulent flows are under investigation statistical analysis needs to be performed.

Utilising the ergodic hypothesis every aeration phase[6] is treated as a separate realisation. The experiment was executed for around one hour with an aeration time of 78 seconds which results in 23 realisations for ensemble averaging. This leads to good statistically converged data.

The temporal resolution of the Point-Grey camera was chosen to only 12 Hz due to the need of storing the huge amount of data directly to a hard drive. For a simple integration of the magnification camera data into the global view the framerate was chosen as a common multiple. The Grasshopper camera has a resolution of 2048x2048 pixel and is monitoring an area of 512x512mm which results in a scaling ratio of 4 px/mm.

The seeding density was set to 0.013 g/l giving barely enough tracers per interrogation window (approx. 10 Tracer/it.win.) to reduce spurious vectors like reported in Keane and Adrian 1992 while minimizing the influence of bubble mobility due to tracer accumulation on the front bubble-surface. The deionized water temperature was equal to the environmental temperature of 297 K with a conductivity of 16.4 µS/cm.

[4] Since the bubbles are rather big (>3mm) they appear not spherical anymore. However, the reported diameters herein are intentionally not Saulter-Mean-Diameters etc. because only 2d size information was available. The size mentioned here is the length of the major axis of the ellipse.

[5] Otherwise the Nd:YAG laser pulses would illuminate every third frame with a higher intensity.

[6] One aeration phase is defined as the time between activating and deactivating an aeration plug.

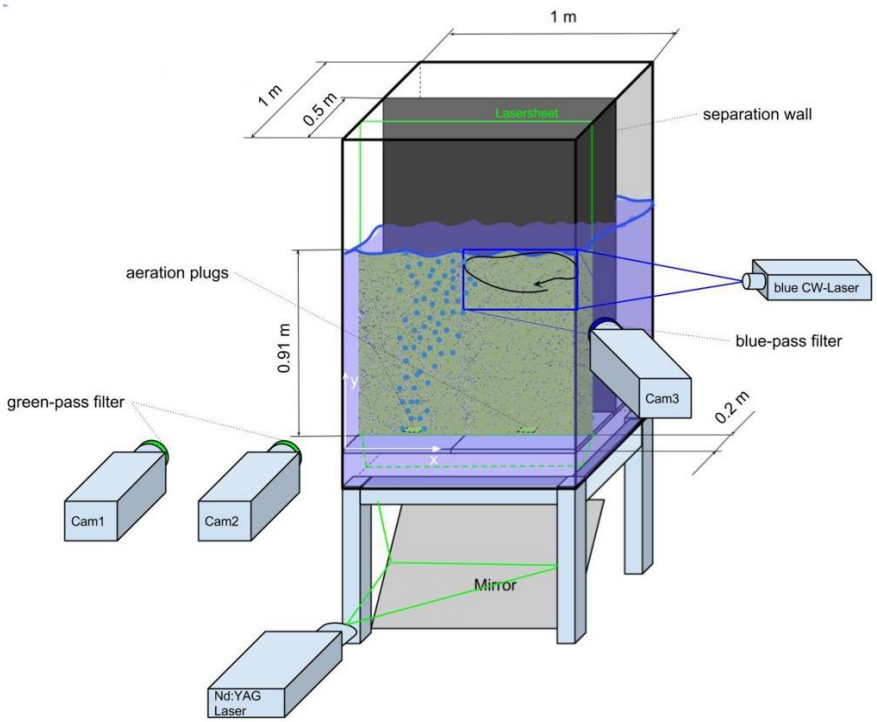

Fig. 3: Experimental setup with alternating aeration. Cam1 and Cam2 (Imager Intense) acquiring complete scene while Cam3 (Point-Grey) acts as a magnification lens for detailed data in a special area of interest.

Phase Separation:

To reduce the amount of spurious vectors within the PIV algorithm the two phases (liquid/gas) need to be separated. This was done by post-processing steps within MATLAB. These steps were:

- Adjusting the contrast of each image that 1% of data is saturated at low and high intensities.
- Converting this image to black and white using a threshold computed with the method of Otsu 1979.
- Suppressing tracer particles by applying a median filter with a windowsize of 4x4 pixel (for Cam1 and Cam2) and of size 15x15 pixel for the magnification camera (Cam3).
- The so generated mask is then dilated with a structuring element of 3 pixel in size to close small gaps and ensure the mask is of sufficient size.
- All the previous steps are performed also for the second correlation frame of the dedicated camera.
- Both masks are added together to a bigger mask which is then applied to each correlation frame. This step is necessary to prevent the mask from changing between the two frames which would lead to spurious vectors again.
- In a final step all images are saved and supplied to LaVisions DaVis software for PIV and PTV computation of the fluid- and gas-phase respectively.

Note that the data in the direct vicinity of the bubbles is lost due to the masking process. Since this research focuses on the turbulent flow structures and their interaction this data loss is considered to be acceptable.

Post-Processing and Analysis:

The velocity vectors computed with DaVis were reimported into MATLAB for further analysis of the turbulent parameters. Therefore, the ensemble average was computed over all aera-

tion phases yielding the time dependent mean- and fluctuating velocities utilising Reynolds decomposition $U = \overline{U} + u'$. Here U denotes the total velocity, $\overline{U}$ the ensemble mean velocity and u' the fluctuating velocity. Obviously, the total velocity is dependent on time, realisation and spatial position. The ensemble averaging procedure reduces the dependent variables of the mean velocity to time and spatial position.
On the basis of this separation the kinetic energy E, the kinetic energy spectrum $\emptyset$, and the turbulent length and time scales are calculated. Since there are various definitions of the turbulent length and time scales reported in the literature they are defined herein as the separation in spatial position or time respectively at which the correlation function ρ reduces to 0.8 the first time. ρ is defined as

$$\rho = \frac{\overline{u_1{}' u_2{}'}}{\sqrt{\overline{u'^2_1}}\sqrt{\overline{u'^2_2}}}$$

with $u_1{}'$ as the analysed fluctuation velocity component of the first spatial/time point and $u_2{}'$ is the fluctuation velocity component of the separated point. By increasing the separation the correlation will rapidly drop from 1 (=fully correlated) to the value of 0.8 which denotes the desired definition of length and time scale. Note that the mean is calculated over the ensemble again and not over time.

Results, Discussion and Conclusion

As a representative example for the phase separation algorithm every step is illustrated in Fig. 4 for the data acquired with Cam1 (left side of the global view). This postprocessing strategy also takes care of some blooming artefacts which can be found at the lower left corner of this image. The generated mask is in good agreement with the appearing bubbles and a dramatic decrease of spurious vectors is achieved. It is self-evident that this approach is only applicable if the tracers are rather small compared to the bubble size and needs to be adjusted for changed optical parameters (e.g. changes which results into bigger captured tracer particles).
The overall procedure enables the fully autonomic processing of each camera (faster processing times due to parallel processing possibility) with consecutively merging utilising calibration images[7] like depicted in Fig.5. Unfortunately, the exposure time of the magnification cam was chosen to long and therefore the tracers are blurred in the prevailing example. Furthermore, the time resolution could be increased by storing the data onto a solid state drive while acquisition or by reducing the time of acquisition to temporary store overflow data within RAM.
By placing the magnification cam to any area of interest the time and spatial resolution can be locally increased dramatically while maintaining the global flowfield. Especially in turbulent flows high velocity gradient regions appear prevalently requiring a high spatial and time resolution for adequate analysis. The interaction with the global flow forms a fundamental boundary condition and needs to be captured simultaneously to build a consolidate basement for simulation validation. The illustrated procedure and its subsequent turbulent analysis tool[8] will provide statistical convergent data with feasible accuracy levels to be compared with for example Large Eddy simulations.
The analysis of all camera data, the extracted turbulent parameters and there interaction can serve as a guideline for adjusting the aeration frequency in the real process to achieve even more efficient rinsing of the liquid metal. Furthermore, by investigating the aeration plug position the erosion of the refractory material may be reduced significantly.

[7] Information of the camera positions and mapping areas
[8] just rarely mentioned herein

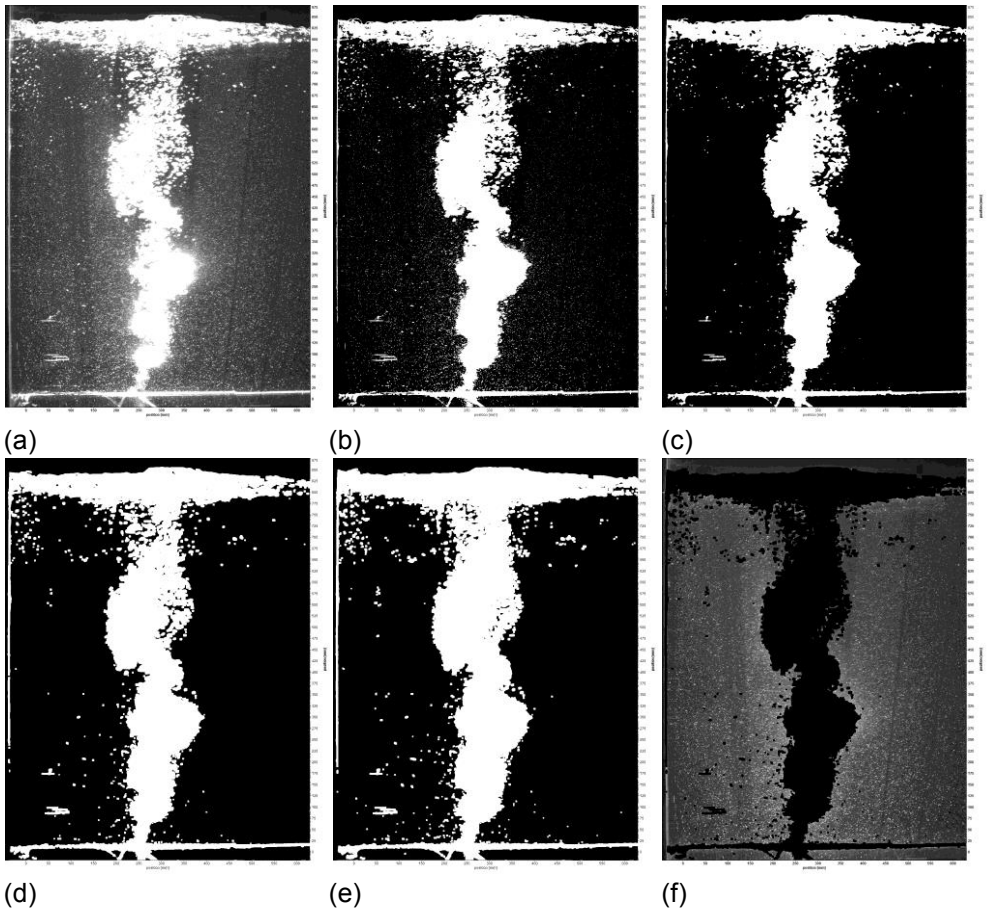

Fig. 4: Post processing scheme. (a) original Image, (b) b/w image computed using Otsu, (c) Tracer removed with median filter, (d) dilated mask, (e) mask fusion of frame 1 and frame 2, (f) applying mask yields resulting image.

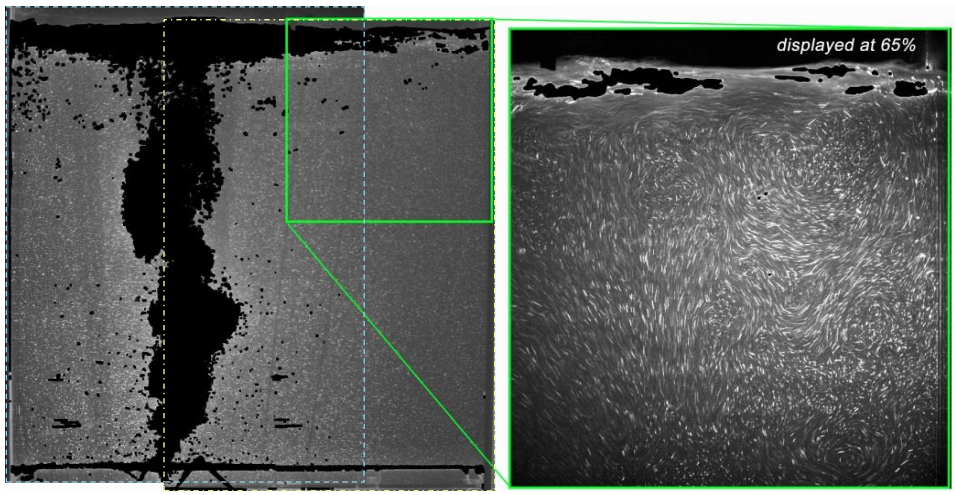

Fig. 5: Fused images. Magnification cam is displayed at 65% relative to global view

Literature

Becker, S., Bie, D., Sweeney, J., 1999: "Dynamic flow behavior in bubble columns", Chemical Engineering Science 54, pp. 4929-4935

Belden, J., Ravela, S., Trucscott, T. Techet, A., 2012: "Three dimensional bubble field resolution using synthetic aperture imaging: application to a plunging jet", Experiments in Fluids, DOI: 10.1007/s00348-012-1322-4

Boyer, C., Duquenne, A., Wild, G. 2002: "Measuring techniques in gas-liquid and gas-liquid-solid reactors", Chemical Engineering Science 57, pp. 3185-3215

Brenn, G., Braeske, H., Durst, F., 2002: “Investigation of the unsteady two-phase flow with small bubbles in a model bubble column using phase-Doppler anemometry”, Chemical Engineering Science 57, pp. 5143-5159
Bröder, S., Sommerfeld, M., 2002: “An advanced LIF-PIV system for analysing the hydrodynamics in a laboratory bubble column at higher void fractions”, Experiments in Fluids 33, pp. 826-837, DOI 10.1007/s00348-002-0502-z
Bröder, D., Sommerfeld, M., 2007: “Planar shadow image velocimetry for the analysis of the hydrodynamics in bubbly flows”, Measurement Science and Technology 18, pp. 2513-2528,
Brücker, C., 1999: “3-D Measurements of bubble motion and wake structure in two-phase flows using 3-D Scanning PIV and stereo-imaging”, Springer Verlag, Developments in Laser Techniques and Applications to Fluid Mechanics
Chen, W., Hasegawa, T., Tsutsumi, A., Otawara, K., 2001: “Scale up effects on the time averaged and dynamic behavior in bubble column reactors.”, Chemical Engineering Science 56, pp. 6149-6155
Deen, N., Hjertager, B., Solberg, T., 2000: “Comparison of PIV and LDA measurement methods applied to the gas-liquid flow in a bubble column”, Proccedings of the 10th Int. Symp. on Appl. of Laser Techniques to Fluid Mech., Lisbon, Portugal
Delnoij, E., Kiupers, J., Swaaij, V., Westerweel, J., 2000: “Measurement of gas-liquid two-phase flow in bubble columns using ensemble correlation PIV”, Chem. Eng. Science 55, pp. 3385-3395
Devanathan, N., Mosleimian, D., Dudukovic´, M.P., 1990: “Flow mapping in bubble columns using CARPT”, Chemical Engineering Science 45, pp. 2285-2291
Devanathan, N., 1991: “Investigation of liquid hydrodynamics in bubble columns via computer automated radioactive particle tracking”, Ph.D. thesis, Washington University in St. Louis USA
Elkins, C.,Alley, M., 2007: “Magnetic resonance velocimetry: applications of magnetic resonance imaging in the measurement of fluid motion.”, Experiments in Fluids 43, pp. 823-858
Garnier, C., Lance, M., Marié, J., 2002: “Measurement of local flow characteristics in buoyancy driven bubbly flow at high void fraction”, Experimental Thermal and Fluid Science 26, pp. 811-815
Huang, S, Plaskowski, A., Xie, C., Beck, M., 1988: “Capacitance based tomographic flow imaging system”, Electron. Lett. 24 (7), pp. 418-419
Huang, S, Plaskowski, A., Xie, C., Beck, M., 1989: “Tomographic imaging of two-component flow using capacitance sensors”, Journal of Physics Engineering Science Insturmentation 22 , pp. 173-177
Keane, R.D., Adrian, R.J., 1992: “Theory of cross-correlation of PIV images”, Applied Scientific Research, Volume 49, pp. 191-215
Kumar, S.B., Moslemian, D., Dudukovic, M.P., 1996: “A gamma-ray tomographic scanner for imaging voidage distribution in two-phase flow systems.”, International Journal of Multiphase Flow, Volume 22, pp. 108-108(1), Supplement 1
Kulkarni, A., Ekambara, K., Joshi, J., 2007: “On the development of flow pattern in a bubble column reactor: Experiments and CFD”, Chemical Engineering Science 62, pp.1049-1072
Kück, U., Schlütter, M., Räbiger, N., 2009: „Analyse des grenzschichtnahen Stofftransports an frei aufsteigenden Gasblasen (Masstransport analysis at free rising gas bubbles)“, Chemie Ingenieur Technik 81, No.10, DOI: 10.1002/cite.200900034
Lain, S., Bröder, D., Sommerfeld, M., 1990: “Experimental and numerical studies of the hydrodynamics in a bubble column”, Chemical Engineering Science 54, pp. 4913-4920
Lin, J.S., Chen, M.M., Chao, B.T., 1985: “A novel radioactive particle tracking facility for measurement of solids motion in gas fluidized beds”, AIChE Journal 31, page 465 ff
Lindken, R., Merzkirch, W., 2002: “A novel PIV technique for measurements in multiphase flows and its application to two-phase bubbly flows”, Experiments in Fluids 33, pp. 814-825,
Mudde, R., Groen, J., Van Den Akker, H., 1998: “Application of LDA to bubbly flows”, Nuclear Engineering and Design 184, pp. 329-338
Mudde, R., Saito, T., 2001: “Hydrodynamical similarities between bubble column and bubble pipe flow”, Journal of Fluid Mechanics, pp. 203-228
Otsu, N.,1979: "A Threshold Selection Method from Gray-Level Histograms," IEEE Transactions on Systems, Man, and Cybernetics, Vol. 9, No. 1, pp. 62-66
Sathe, M., Thaker, I., Strand, T., Joshi, J., 2010: “Advanced PIV/LIF and shadowgraphy system to visualize flow structure in two-phase bubbly flows”, Chemical Engineering Science 65, pp. 2431-2442
Seeger, A., Affeld, K., Goubergrits, L., Kertzscher, U., Wellnhofer, E., 2001: “X-ray-based assessment of the three-dimensional velocity of the liquid phase in a bubble column”, Experiments in Fluids 31, pp. 193-201
Tokuhiro, A., Maekawa, M., Iizuka, K., Hishida, K., Maeda, M., 1998: “Turbulent flow past a bubble and an ellipsoid using shadow-image and PIV techniques”, International Journal of Multiphase Flow 24, pp. 1383-1406